

Failure Analysis of Base Plate Bolts of Radial Forging Machine

K. Aliakbari*

Mechanical Engineering Department, Faculty of Montazeri, Khorasan Razavi Branch, Technical and Vocational University (TVU), Mashhad, Iran.

Article info

Article history:

Received 10 August 2019

Received in revised form

10 September 2019

Accepted 17 September 2019

Keywords:

Radial forging machines

Bolts failure

Microstructure

Mechanical properties

Stress analysis

Abstract

In this study, the failure analysis of base plate bolts of radial forging machine is investigated. Premature failure had occurred from the bolts shank-head fillet and threads zones. Hardness, impact and tensile tests are carried out to investigate the mechanical properties and spectrophotometer is used to evaluate the bolts chemical composition. Optical Microscope (OM) and Scanning Electron Microscope (SEM) are used for the investigation of microstructure, defects, fracture surface and failure causes. The fracture surface morphology shows that the crack growth consisted of bolts shank-head fillet and threads zones including the initiation zone, fatigue crack growth zone along with the beach marks and ratchet steps and the rapid final fracture zone. Stress analysis shows that the amount of pre-tightening selected lower than the proposed value leads to the joint loosening and shortens the bolt's fatigue life. In addition, based on the paper results, the existing flowchart for component fabrication is analyzed and a flowchart based on research field is presented to enhance the quality of radial forging machine parts.

1. Introduction

Radial forging machines usually have four hammers designed to forge the longitudinal workpiece. The drive system of hammers is either a mechanical or a hydraulic type. Radial forging machines with mechanical actuators are used for cold forging of small sections. Radial forging machines with hydraulic actuators are used for hot forging of large sections. The four pumps are driven by a motor that is coupled directly to the pressure cylinders and apply force to the hammers through the push rod. In a radial hydraulic forging machine, billets are squeezed by hammers in four directions and then workpiece is fed and rotated as in Fig. 1. The hammers are mounted on the base plate by two clamps and the base plate is mounted on the thrust ring by bolts. The thrust ring also serves as an intermediary between the connecting rod and the base plate [1-2].

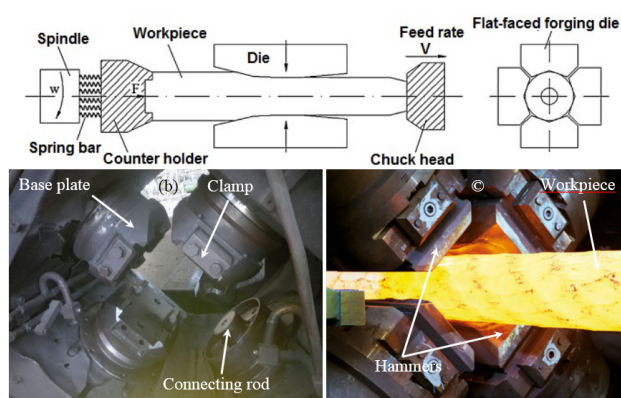


Fig. 1. Radial forging machine: a) Schematic operation, b) Drive system of hammers, c) Forged workpiece.

Li and Wang [3] investigated the failure analysis of the connection bolts of the nuclear power worm gear. Their results showed that failure was due to

*Corresponding author: K. Aliakbari (Assistant Professor)

E-mail address: Karim.aliakbari@gmail.com

<http://dx.doi.org/10.22084/jrstan.2019.20037.1112>

ISSN: 2588-2597

two-way bending fatigue failure. Decreasing the surface of the bolts and the stress concentration on the bolt thread neck reduced the fatigue strength of this position and resulted in the initiation of the fatigue cracks. By comprehensive analysis and stress estimation, it was also concluded that the main reason for the bolt fracture was due to the big gap between the bolts and the bolt positioning hole which resulted in the fatigue fracture of the bolts. Kong et al. [4] investigated the failed U-shaped bolts during the vehicle test. The cause of failure was examined using the tests of dimensional, macro-micro observation, metallographic, hardness and tensile property. The results indicated that U-shaped bolts and nuts were fatigue fracture. The failure of the U-shaped bolts and nuts was due to the presence of densely distributed surface micro-cracks, small dimensions, surface decarburization appearance and low strength of materials. Pilone et al. [5] examined the bolt connections failure used to hold the lights in the tunnels of a highway. Past research has shown that failure is due to a deep corrosion process, with sodium chlorides sprayed inside tunnels during winter to prevent freezing of the road. Previous studies have also indicated that corrosion only affects the bolts, while all other components of the joints are intact. The EDS analysis indicated that stainless steel bolts were of copper type, which did not have a relatively good corrosion resistance. Behjati et al. [6] investigated the failure analysis of the U-bolts of car wheel retainers. Their study showed that the high carbon and boron content in the U-bars increased the precipitation of boron-containing carbides along the grain boundaries. These sediments act as neutralization sites for cracks and are responsible for fracture under straight-phase stresses. Based on the results, an optimal temperature is proposed for the Y source segments to solve the problem. Molaei et al. [7] reviewed the failure of the sixteen connecting bolts of a filter press cylinder-piston system. They examined the state of bolt stress during service conditions and the failure causes were obtained from analysis of fracture and data. According to the results, they concluded that the bolts were broken by fatigue mechanism. It seemed that inadequate torque was used during the assembly process. Casanova and Mantilla [8] examined the failure of bolts used to connect the turbine to the shaft of a hydroelectric power generator. Three bolts out of the ten bolts were broken during the disassembly process to replace the turbine. The results indicated that some of the scratches in the roots of the thread produced during the machining process and then corrosion during the working operation significantly affected fatigue life. Jeong et al. [9] investigated the processes of joining and releasing bolt in joining bolts with different thickness and strength using finite element method. Their results showed that in order to resolve thread failure, the depth of connection should be chosen as low as possible.

The present study investigates the failure cause of

radial forging machine base plate bolts working under cyclic force. Hardness, impact and tensile tests are carried out to investigate the mechanical properties and spectrophotometer is used to evaluate the chemical composition of the bolts. Optical Microscope (OM) and Scanning Electron Microscope (SEM) are used for the investigation of microstructure, defects, fracture surface and failure causes.

In most of the previous studies, the focus was on evaluating the mechanical properties of the bolt material, investigation of the microstructure of the bolt material, fractography of the fracture surface and failure analysis of bolts. Stress analysis of bolt, however, has received less attention. In summary, the innovations and objectives of the current study can be expressed as follows:

- Preparing experimental measurements on failure analysis including mechanical properties (hardness and tensile test), chemical composition of material and microstructure of material using Optical Microscope (OM) and fractography of fracture surface using Scanning Electron Microscope (SEM).
- Analyzing the stress of broken bolts and comparing them with the proposed model.
- Analyzing the failure cause and offering suggestions.
- Suggesting the algorithm of manufacturing process and parts failure detection.

2. Experimental Study Method

The chemical composition of the base plate bolts of Radial Forging Machine is tested according to ASTM E415-14 & ASTM E1086 [10-11] standard by SPECTROMAXx manufactured by Germany.

The geometric dimensions of the bolts are measured using the Micrometer and Vernier Caliper of the Mitutoyo Corporation of Japan. Macroscopic observations are done using a Samsung 8MP AF camera with a $1.22\mu\text{m}$ pixel size.

To examine the hardness and microstructure, a cross-section of bolt with the thickness of 15mm is cut by the EDM machine and then is machined from both sides. The surface of the samples is then finished with sandpapers no. 60 to no. 1200, and for final polishing, diamond paste is used. Surface polishing is done by aqueous solution of Al_2O_3 and then is etched with 2% Nital. Alcohol washing and hot air drying are used as the final step of polishing. Then, microscopic images are made using Optical Microscope (OM) from different areas of the bolt cross section. Finally, hardness test is run according to standard ASTM: E384-11e1 with a hardness measurement device with 30kg force is applied for 10 seconds.

For evaluating the mechanical properties of the bolt material, such as ultimate stress (US), yield stress (YS) and elongation, test samples are machined by a CNC lathe. The samples are then tested in accordance with the standard ASTM E8M-97a and reference [12-13] by test machines. The results of the experiment are stored at the sampling rate 2 times per second in the form of force-displacement. The length variation of the specimens is measured by an extensometer with a length of 50mm. In order to perform the test, the motion speed of the machine grips is set at 0.50 millimeter per minute.

For evaluating the toughness property of the bolt material, the Charpy Impact Test specimen is cut in accordance with Standard ASTM A370 [14]. The test specimen consists of a bolt material piece, 55×10×10mm having a notch machined across one of the larger dimensions. A V-shaped notch with an angle of 45° and a depth of 0.2mm with a radius of gap 0.25mm is milled from bolts according to the standards and the test specimen is done by Charpy impact test machine.

In order to investigate the fracture surface, the broken bolts are first cut by an EDM machine and the samples are placed in an ultrasonic bath for one hour and then images are made with high magnifications by SEM machine model LEO 145 OVP.

3. Results and Discussion

Table 1 lists the specifications of the radial forging machine. Fig. 2a shows the main components of the radial forging machine involved in the failure, and Fig. 2b shows a healthy bolt, most of which is broken severely from two zones of shank-head fillet and bolt threads.

3.1. Material Properties of Base Plate Bolts

The chemical composition experiments of the constituent elements of the base plate are repeated three times at 24°C and relative humidity of 23%, and the results of mean numbers are weighted in Table 2. The values of the elements specified in the table are equivalent to AISI 4340 steel in American standard AISI and equivalent to DIN1.6580 in German DIN standard.

Table 2

The chemical composition of DIN1.7034 and Standard.

Symbol	Fe	C	Si	Mn	P	S	Cr	Ni	Mo	Al	Cu
DIN1.6580	94.3	0.333	0.357	0.51	0.01	0.006	1.97	1.87	0.332	0.016	0.205
Standard	Base	0.26-0.34	≤0.4	0.5-0.8	≤0.025	≤0.035	1.8-2.2	1.8-2.2	0.3-0.5	-	-

Table 3

Mechanical properties of the DIN1.7034 and Standard alloy.

Symbol	Yield stress (MPa)	Ultimate tensile strength (MPa)	Elongation (%)
Sample	693.56	1080	20.06
Standard alloy	Min. 600	Min. 800	Min. 13
Requested alloy	-	800-950	-

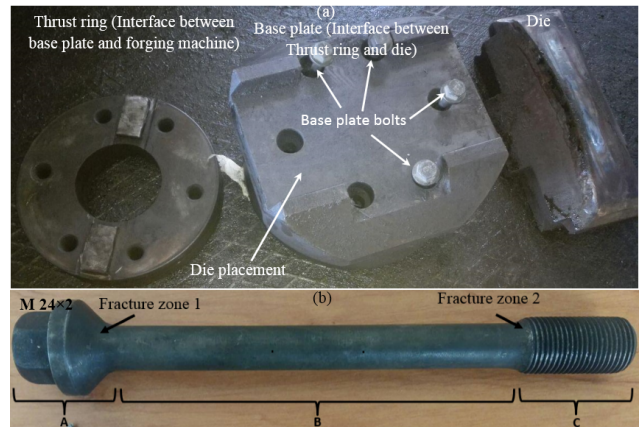


Fig. 2. a) The main components of the radial forging machine involved in the failure, b) Bolt fracture zones.

Table 1

Specification of radial forging machine.

1	Machine model	SXP-25
2	No of Hammers	4
3	Forged workpiece weight (Ton)	1.2
4	Largest initial material dimensions	∅ 250
5	Smallest dimensions forged (mm)	∅ 50
6	Min. forging speed (m/s)	1
7	Max. forging speed (m/s)	12m/s
8	Min. forging length (mm)	2500
9	Max. forging length (mm)	8000
10	Manipulator: Min. diameter (mm)	∅ 50
11	Manipulator: Max. diameter (mm)	∅ 300
12	Forging force of each hummer (Ton)	340
13	Max. forging torque (KN.m)	12

Using the results of the tensile tests, the final strength and length change are measured. The mechanical properties of DIN1.6580 test material for the base plate bolt are listed in Table 3 and the stress-strain curve of the material engineering is drawn in Fig. 3. The first row of Table 3 shows average values of the three tested samples, the second row is standard alloy sample values extracted from the steel handbook and the third row shows values proposed for the manufacture of plate bolts by GFM. Tensile tests performed on the prepared samples indicate that the values obtained are within the acceptable range of the standard alloy and the proposed alloy by GFM.

Using the results of the impact tests, the material toughness and energy absorption during plastic deformation are measured. The test results are listed in Table 4. In addition, this test is used to check the correctness of the heat treatment and also to determine the sensitivity of the steels to the precipitation hardening and the brittleness from the temper. The impact tests performed on the prepared samples show that the obtained values are acceptable.

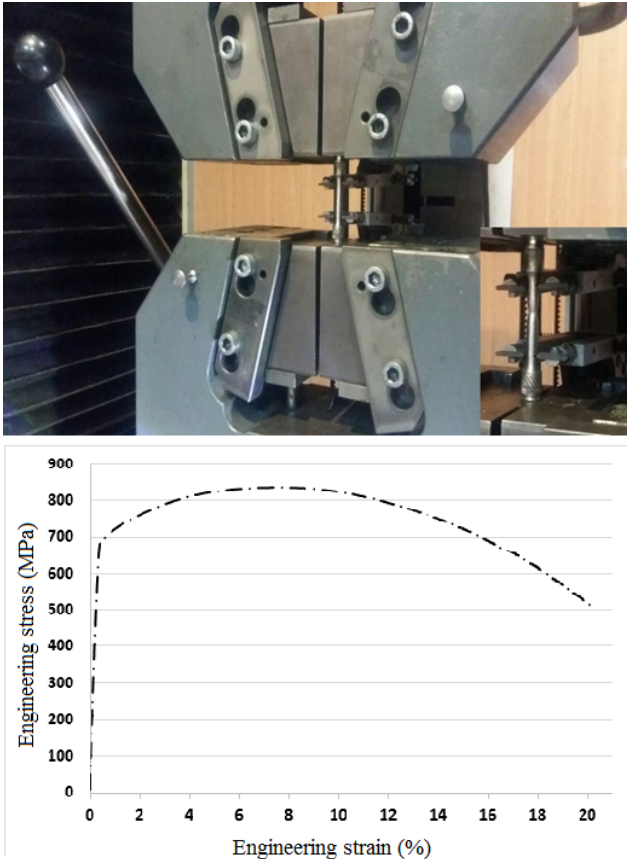


Fig. 3. a) Test machine with tensile specimen and extensometer, b) Engineering stress–strain curves of DIN1.7034 steel.

Table 4
Notch impact energy of the DIN1.6580 and Standard alloy.

Symbol	ISO-V [J] (Kv-20OC)
Sample 1	157.6
Sample 2	194.5
Sample 3	168.8
Standard alloy	Min. 27

3.2. Hardness and Optical Micrographs

The micrographs of the base plate bolts examined are shown using optical microscopes in Fig. 4. It is seen that the structure of the base plate bolts is of the martensite steel type.



Fig. 4. Microstructure of the cross-sectional area of the base plate bolt after etching with 100× magnification.

First, the hardness test is performed on the cross-sectional area of the specimen by applying 30Kgf force for 10 seconds and the hardness is plotted from center of bolt to bolt outer diameter in Fig. 5. Then the hardness test is performed on wire cut specimen in three different threads. The thread Vickers hardness is measured in points 1 to 3 of Fig. 5 in accordance with the requirements of Table 18 of ISO 898-1: 2009 (E) [15]. The test force is selected according to the standard 2.942N (Vickers hardness test HV 0.3). The Vickers hardness value for bolts without carbonization at point 2 according to the standard should be greater than the Vickers hardness at point 1 according to Eq. (1) [15].

$$\text{For decarburization bolts: } HV(2) \geq HV(1) - 30 \quad (1)$$

In Fig. 5, the height of the not carburize zone E, must be in accordance with ISO 898-1: 2009 (E). The measured hardness values of the threads are in accordance with the standard and are valid in Eq. (1). The results of Fig. 5 show that the bolt hardness increases from center to external diameter. The hardness values shown in Fig. 5 and the hardness values of points 1 and 2 of Fig. 5 are within the bolts standard material and, therefore, the heat treatment performed on the bolts is correct, so hardness does not impose any problems in the bolts.

3.3. Fractography of the Fracture Surface

Finding the origin of the crack is the primary goal of fractography science and it is necessary for a proper analysis of the fracture. Initiation and propagation of the cracks make the distinctive signs on the fracture surface, such as beachmarks, radial lines, river signs, radial lines and chevrons that show the growth direction of the cracks. These marks are examined for the

origin of the cracks. The appearance of these marks on the crack surface is a function of tensile loading type, shear, bending, fatigue or torsional, stress state, amount of stress, existence of stress concentration, environmental factors, and material factors [16-17].

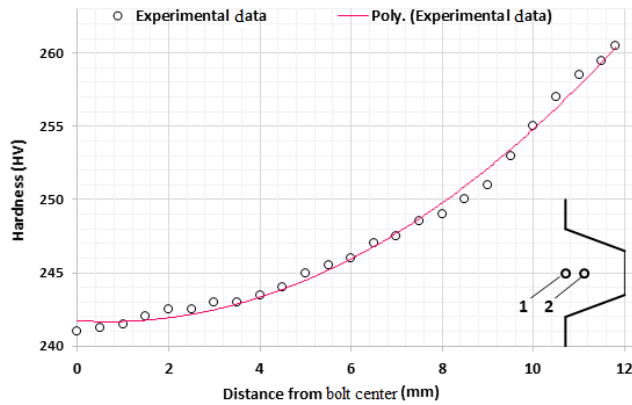


Fig. 5. Hardness distribution from center to outer diameter of the bolt.

Fig. 6 and Fig. 7 show the optical examination of the fracture surface of the bolts, where fatigue has been identified as the main cause of failure with the zones of initial crack initiation A, crack propagation B, and final fast fracture C. Fracture surfaces have radial line and beachmarks that are marks of fatigue failure. The surface is surrounded by ratchet steps, which can be the origin of the initiation of radial lines. The beachmarks and the radial lines are signs of fatigue failure. Further examination of the fractured surfaces of the bolts suggests that the fatigue zone shown in Fig. 6 and Fig. 7 is relatively large and approximately 80% of the total fractured surface.

Fig. 8 and Fig. 9, respectively, show the SEM fracture surface of the initial crack zone of the bolts of Fig. 6 and Fig. 7, respectively. The SEM results also show the effects of fatigue including beachmarks and striations with high magnification. Similar results to the SEM on failure analysis (e.g. [18-19]) of fatigue effects including beachmarks and striations have been reported in fatigue loaded specimens.

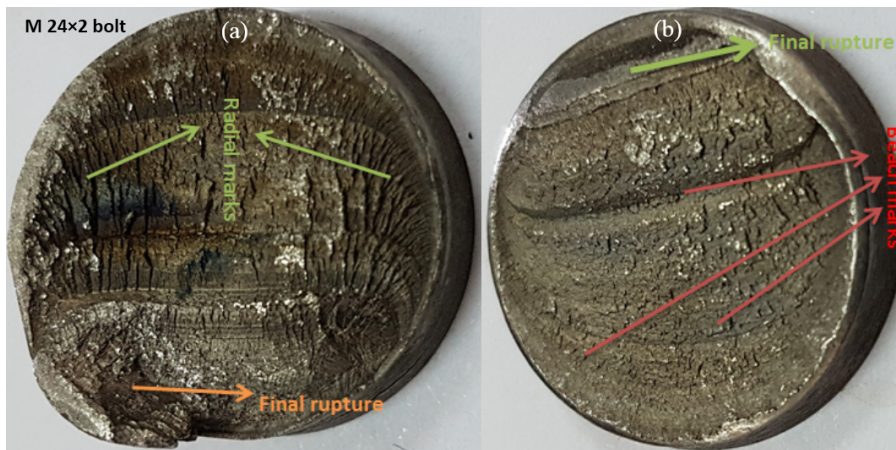


Fig. 6. Macro morphology of fracture surface of the radial forging machine bolts shank-head fillet (zone 1).



Fig. 7. Macro morphology of fracture surface of the radial forging machine bolts threads (zone 2).

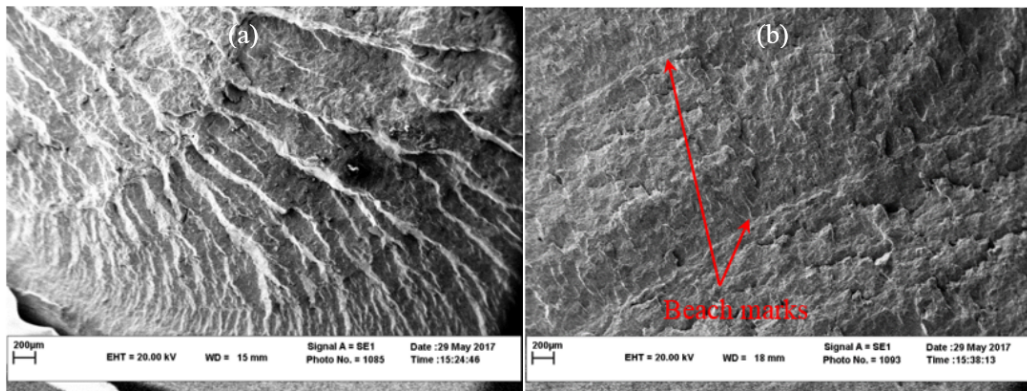


Fig. 8. a) Striations indicating fatigue failure, b) Beach marks indicating fatigue failure.

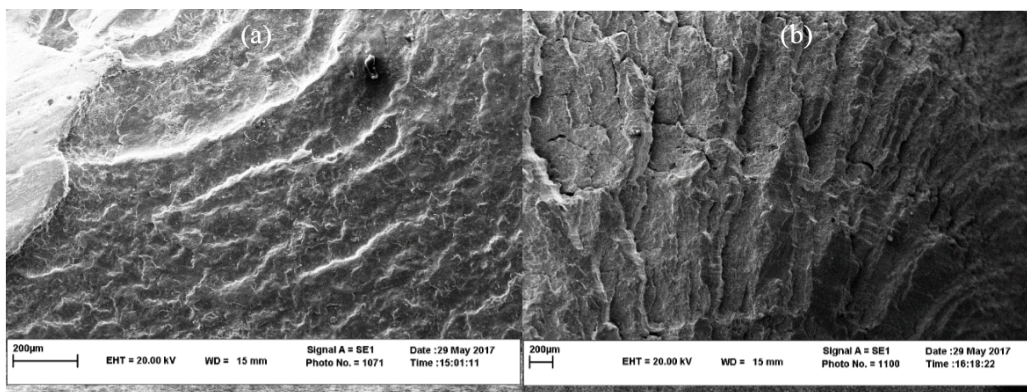


Fig. 9. a) Striations indicating fatigue failure, b) Beach marks indicating fatigue failure.

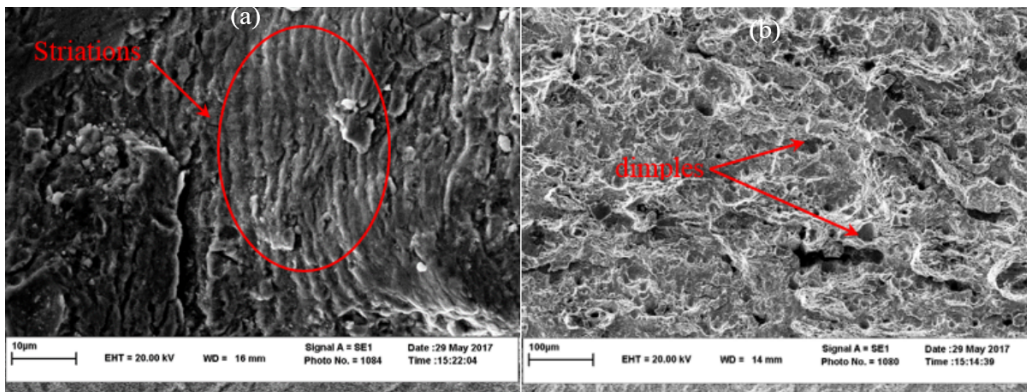


Fig. 10. a) Striations indicating fatigue failure, b) Shear failure.

Fig. 10 shows the SEM fracture surface of the fatigue crack growth zone B and the final fast fracture zone C of the broken bolt Fig. 7a. The averaged distance between the relatively large striations in Fig. 10a is obviously indicative of a low cycle fatigue failure in this study. Fig. 10 shows the SEM fracture surface characterization of the dimple shear fracture features, which is the last cracking step, and the large number of dimples in the fracture propagation zone shows excellent bolt toughness. The results of the impact tests confirm the toughness of the bolt fracture surface. Similar research has been reported on failure analysis (e.g. [20-21]) of fatigue effects including beachmarks and striations in the bolts.

3.4. Stress Analysis

Base plate bolts must withstand high loads to keep the base plate sealed tightly against the thrust ring and connecting rod. Base plate bolts are loaded in tension due to the presence of pre-tightening force F_{PT} and maximum forging force F_F . Fig. 11 [22-23] shows a diagram of force F vs. deformation δ with a pre-tightening F_{PT} and a reaction cyclic loading F_R . It is noted that the value of the reaction force F_R is about 1/10th of the forging force (impact force) of each hammer. In contrast, the duration of the reaction forces lasted for ten times longer than that of the forging force [24-25].

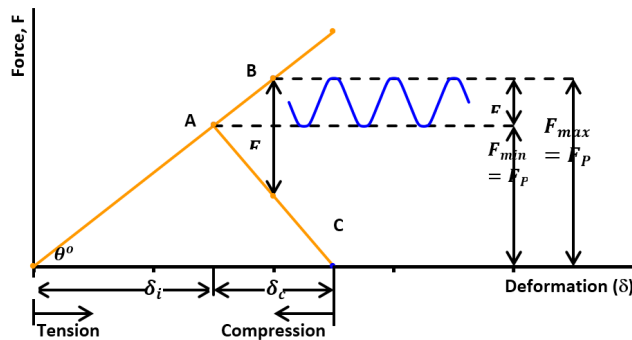


Fig. 11. Diagram representing the beneficial effect of a pre-tightening on bolts.

The cyclic stress amplitude imposed on a bolt is highly dependent on pre-tightening, because if the pre-tightening increases, there is a decreasing cyclic alternating stress σ_a . Lack of adequate pre-tightening promotes premature fatigue, leading to fatigue crack growth under service loading conditions. Table 5 lists calculations of the proposed bolted joint and current work with details. Bowman [26] recommends a pre-tightening of 75 percent of proof load, which is about the same as the RB&W recommendations for the reused bolts.

When the radial forging machine is in operation, the reaction force from forging force leads to increases in the length of the bolt, decreases in the deformation in the base plate and reduces the deformation of the thrust ring. According to M24×2 (bolt size) and 340 Ton (forging force or hummer impact), the pre-tightening stress $\sigma_{min\ CW}$, the pre-tightening

stress+stress amplitude $\sigma_{max\ CW}$ and the stress amplitude $\sigma_{a\ CW}$ are 282.96MPa, 430.35MPa and 73.7MPa, respectively (see Table 5). All three of these current work stresses should be lower than the proposed values, but in this study, the amount of tightening stress is approximately equal to the proposed pre-tightening and the other two are lower than the proposed values. Due to the amount of stress amplitude proposed, it is recommended to use Grade 10.9 bolts with high fatigue strength.

Depending on the type of loading, the proper amount of initial torque (pre-tightening) for bolt tightening also plays a significant role in fatigue life [27]. The initial torque applied to the bolt in the current work is 520Nm and the equivalent stress is 282.96MPa, while the initial torque value for the best lubrication state proposed by FGM is 620Nm and the equivalent stress is 337.38MPa, both of which are lower than the values proposed in Table 5. With too little clamping force, the joint may loosen. If the joint is exposed to cyclical loads, too little clamping force can shorten the bolt's fatigue life [27].

Hence, one of the root cause of failure can be a deficient pre-tightening of the base plate bolts, which could originate a significant alternating stress amplitude. Bolts were going suffering some failure at bolts shank-head fillet and threads zones. It is well-known that cracks generally start at the threads fillet and improper shank-head fillet where the stress concentration is higher. One reliable indication is also revealed by the presence of beachmarks [28-29], as is shown in this failure analysis. For all fractured base plate bolts, the root cause is the same with fatigue marks.

Table 5
Calculations of proposed bolted joint and current work [22-23].

	Proposed	Current work
Preload	$F_{minP} = F_{PT} = 0.75F_P = 0.75 \times 226650.7 = 169988.03\text{N}$	$F_{minCW} = F_{PT} = \frac{T}{k \times d} = \frac{520000}{0.2 \times 23.9} = 108786.6\text{N}$
Maximum load	$F_{maxP} = F_P = 226650.7\text{N}$	$F_{maxCW} = F_{PT} + F_R = 165453.27\text{N}$
Alternating load	$F_{aP} = \frac{F_{maxP} - F_{minP}}{2} = 28331.34\text{N}$	$F_{aCW} = \frac{F_{maxCW} - F_{minCW}}{2} = \frac{F_G}{2} = 28333.33\text{N}$
Preload stress	$\sigma_{minP} = \sigma_i = 0.75S_P = 442.15\text{MPa}$	$\sigma_{minCW} = \frac{F_{minCW}}{A_t} = 282.96\text{MPa}$
Maximum stress	$\sigma_{maxP} = S_P = 589.53\text{MPa}$	$\sigma_{maxCW} = \frac{F_{maxCW}}{A_t} = 430.35\text{MPa}$
Alternating stress	$\sigma_{aP} = \frac{\sigma_{maxP} - \sigma_{minP}}{2} = 73.69\text{MPa}$	$\sigma_{aCW} = \frac{\sigma_{maxCW} - \sigma_{minCW}}{2} = 73.7\text{MPa}$
Considerations	Minor diameter: $d_r = d - 1.226869p = 24 - 1.226869 \times 2 = 21.55\text{mm}$	
	Mean diameter: $d_m = d - 0.649519p = 24 - 0.649519 \times 2 = 22.7\text{mm}$	
	Effective tensile stress area: $A_t = \frac{\pi}{4} \left(\frac{d_m + d_r}{2} \right)^2 = 384.46\text{mm}^2$	
	Proof stress: $S_P = 0.85 \times S_P = 0.85 \times 693.56 = 589.53\text{MPa}$	
	Proof load: $F_P = S_P \times A_t = 589.53 \times 384.46 = 226650.7\text{N}$	
	Pre-tightening: $F_{PT} = \frac{T}{k \times d} = \frac{520000}{0.2 \times 23.9} = 108786.61\text{N}$	
	Reaction force: $F_R = 34\text{Ton}$	

3.5. Algorithm of Manufacturing Process and Parts Failure Detection

Parts wear is one of the most important problems in the mining and industrial sector where wear in critical situations can cause failure. One solution is to manufacture new parts and replace them with worn parts, but this choice is largely costly. Another method is repair welding of the parts by welding and then machining [30]. The solid arrow in flowchart (Fig. 12) shows how to fabricate the forging machine parts in the steel complex. To improve the quality of the radial forging machine parts, the dashed line section of the algorithm is developed to show feedback on the broken parts. The present algorithm includes drawing parts and manufacturing process (from raw material step to final machining step), material selection, initial cutting to roughness dimensions, rough machining to parts geometry with different machine tools (lathe, milling, grinding, etc.), removing sharp edges to eliminate thermal stress concentration, heat treatment of the parts to the desired hardness, final machining and grinding, and closing parts on machine. After the radial forging machine has been operated and the sound has been created by the machine, there are two modes: the clearance caused by wear that needs repair and the part is reused or the part failure that is discarded. For improvement of the bolts quality, the fatigue life and the investigation of failure cause are added to the new algorithm. Due to the sleep of the radial forging machine and the high cost of fabrication of the parts, this method is suggested as the least costly method for improving the parts.

3.6. Cause Investigation of Bolts Failure

Due to the performance of the base plate bolts, they are subject to severe impact and cyclic loads. The amount of initial torque to tighten the bolt also plays a significant role in fatigue life. The initial torque applied to the bolt in the current work is 520Nm and the equivalent stress is 282.96MPa, while the initial torque value for the best lubrication state proposed by FGM is 620Nm and the equivalent stress is 337.38MPa, both of which are lower than the values proposed. The bolts in a tension joint must act like clamps. The tightening of the bolt and nut produces a tensile pre-stress, which is approximately equal to the compressive stress introduced in the joint material. The behavior and life of the joint depends on how tightly the bolts clamp and how long they can maintain their preload. Therefore, the initial torque is low and there is a clearance in the joints that causes wear and failure on the bolts over time. With too little clamping force, the joint may loosen. If the joint is exposed to cyclical loads, too little clamping force can shorten the bolt's fatigue life. Hence, one of the root cause of failure can be a deficient

pre-tightening of the base plate bolts, which could originate a significant alternating stress amplitude. Proper torque is applied when tightening the bolt, causing the bolt to approach the yield point (less than the yield) and to lock in place.

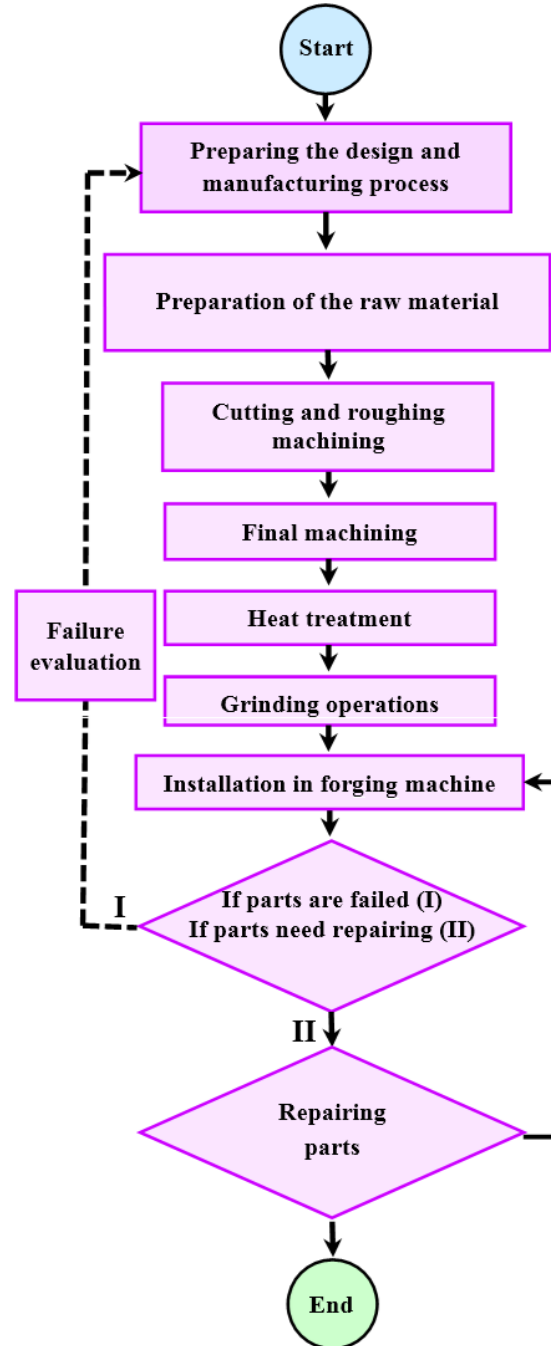


Fig. 12. Flowchart of the manufacturing process and parts failure detection.

In this case, the longest service life of the bolts is expected. Also, the initial torque should be visited at certain times because the initial pre-load of the bolt may be lowered due to relaxation, which may be less noticeable. In addition, the proper amount of fillet radius plays an important role in the concentration of stress between the shank and the bolt head, which, ac-

ording to the findings of past research, is not applied very accurately. Finally, the bolt production method must be forged and threaded by rolling after heat treatment. The use of rolling thread after heat treatment results in better surface quality and lower surface defects. Therefore, choosing the proper material, the bolt manufacturing process, the pre-tightening torque, the amount of fillet between bolts shank-head, and the lubricant are important parameters. Due to the amount of stress amplitude proposed, it is recommended to use Grade 10.9 bolts with high fatigue strength.

4. Conclusions and Suggestions

In the present study, the failure of radial forging bolts is investigated. Failure occurred in the bolts shank-head fillet and threads zones. In this paper, the mechanical properties (tensile and hardness test), chemical composition, microstructure and fractography are first determined. These studies have helped to improve practical structural specimens and have proven to be useful for the proper design of new specimens. The results of this study can be expressed in the following framework:

1. Bolt grade is first determined according to ISO 898-1. According to the results of the tensile test, the bolts are in the dominant grade of 8.8, which means a minimum tensile strength of 800 MPa and a minimum yield strength of 640MPa. Also, the chemical composition and impact test results confirm the grade of 8.8 bolts.
2. Fracture cross-sectional images as well as SEM images show fatigue occurrence, which is one of the most common causes of failure in bolt joints. The bolt failure mode according to the SEM images is the low fatigue cycle failure. The morphology of the fracture surfaces shows that the crack growth consisted of a smooth and uniform surface along the beachmarks, ratchet steps zone with the river cracks, and fast final fracture zone.
3. Stress analysis shows that the amount of stress amplitude is approximately equal to the proposed value but pretension and maximum stress are lower than the proposed values. Due to the initial torque amount of current work is selected less than the amount proposed by manufacture. This decreases clamping force, and therefore, causes the joint loosening. As a result, the joint is exposed to cyclical loads, too little clamping force shorten the bolt's fatigue life. Due to the amount of stress amplitude proposed, it is recommended to use Grade 10.9 bolts with high fatigue strength.
4. Due to the type of loading, the amount of initial torque for bolt fastening also plays a significant role in fatigue life. The initial torque applied to the bolt in the oil-impregnated state was 520Nm, while the initial torque for the best lubrication state (i.e., friction coefficient 0.1) is 620Nm. Also, the fillet radius has a significant role in the concentration of stress between the shank and the bolt head. In addition, the bolt production method must be forged and threaded by rolling after heat treatment. Finally, the use of rolling thread after heat treatment results in better surface quality and lower surface defects.

References

- [1] G.D. Lahoti, L. Liuzzi, T. Altan, Design of dies for radial forging of rods and tubes, *J. Mech. Work. Technol.*, 1(1) (1977) 99-109.
- [2] J. Chen, K. Chandrashekhara, C. Mahimkar, S.N. Lekakh, V.L. Richards, Study of void closure in hot radial forging process using 3D nonlinear finite element analysis, *Int. J. Adv. Manuf. Technol.*, 62(9-12) (2012) 1001-1011.
- [3] L. Li, R. Wang, Failure analysis on fracture of worm gear connecting bolts, *Eng. Fail. Anal.*, 36 (2014) 439-446.
- [4] H. Kong, D. Liu, T. Jiang, U-shaped bolts fracture failure analysis, *Procedia Eng.*, 99 (2015) 1476-1481.
- [5] D. Pilone, A. Brotzu, F. Felli, Failure analysis of connecting bolts used for anchoring streetlights of a mountain highway, *Eng. Fail. Anal.*, 48 (2015) 137-143.
- [6] P. Behjati, A.R. Etemadi, H. Edris, Failure analysis of holding U-bolts of an automobile wheels, *Eng. Fail. Anal.*, 16(5) (2009) 1442-1447.
- [7] S.H. Molaei, R. Alizadeh, M. Attarian, Y. Jaferian, A failure analysis study on the fractured connecting bolts of a filter press, *Case Stud. Eng. Fail. Anal.*, 4 (2015) 26-38.
- [8] F. Casanova, C. Mantilla, Fatigue failure of the bolts connecting a Francis turbine with the shaft, *Eng. Fail. Anal.*, 90 (2018) 1-13.
- [9] J.H. Jeong, H.K. Lee, K. Park, J.B. Kim, An investigation into the anti-releasing performance of a serrated bolt, *J. Mech. Sci. Technol.*, 29 (12) (2015) 5127-5132.
- [10] ASTM E415-14, Standard Test Method for Analysis of Carbon and Low-Alloy Steel by Spark Atomic Emission Spectrometry, ASTM International, West Conshohocken, (2014).

- [11] ASTM E1086-14, Standard Test Method for Analysis of Austenitic Stainless Steel by Spark Atomic Emission Spectrometry, ASTM International, West Conshohocken, (2014).
- [12] K. Aliakbari, K.H. Farhangdoost, Plastic deformation influence on material properties of autofrettagged tubes used in diesel engines injection system, *J. Pressure Vessel Technol.*, 136(4) (2014) 041402.
- [13] K. Aliakbari, Kh. Farhangdoost, The investigation of modelling material behavior in autofrettagged tubes made from aluminium alloys, *Int. J. Eng.*, 27(5) (2014) 803–810.
- [14] ASTM A370-19, Standard Test Methods and Definitions for Mechanical Testing of Steel Products, Sections 20-30, (2019).
- [15] ISO 898-1:2013 (en), Mechanical properties of fasteners made of carbon steel and alloy steel- Part 1: Bolts, bolts and studs with specified property classes - Coarse thread and fine pitch thread, (2013).
- [16] ASM Metals Handbook, Volume 12: Fractography, Second Printing, ASM International Publisher, (1987).
- [17] K. Aliakbari, The analysis of light-duty truck diesel engine crankshaft failure, *J. Stress Anal.*, 2(2) (2018) 11-17.
- [18] M. Bernabei, L. Allegrucci, M. Amura, Chapter 5: Fatigue failures of aeronautical items: Trainer aircraft canopy lever reverse, rescue helicopter main rotor blade and fighter-bomber aircraft ground-attack main wheel, *Handbook of Materials Failure Analysis with Case Studies from the Aerospace and Automotive Industries*, (2016) 87-116, DOI: 10.1016/B978-0-12-800950-5.00005-3.
- [19] F. Belben, Chapter 6: Failure investigations of helicopter tail rotor gearbox casings at Agustawestland Limited, *Handbook of Materials Failure Analysis with Case Studies from the Aerospace and Automotive Industries*, (2016) 117-146, DOI: 10.1016/B978-0-12-800950-5.00006-5.
- [20] Z. Yu, X. Xu, Chapter 17: Failure analysis cases of components of automotive and locomotive engines, *Handbook of Materials Failure Analysis with Case Studies from the Aerospace and Automotive Industries*, (2016), DOI: 10.1016/B978-0-12-800950-5.0.
- [21] X. Zhu, J. Xu, Y. Liu, B. Cen, X. Lu, Z. Zeng, Failure analysis of a failed connecting rod cap and connecting bolts of a reciprocating compressor, *Eng. Fail. Anal.*, 74 (2017) 218-227.
- [22] R.G. Budynas, J.K. Nisbett, Shigley's, Chapter 8: Mechanical Engineering Design, 9th edition, McGraw Hill Publisher, (2012).
- [23] M. Fonte, L. Reis, V. Infante, M. Freitas, Failure analysis of cylinder head studs of a four stroke marine diesel engine, *Eng. Fail. Anal.*, 101 (2019) 298-308.
- [24] J. Sun, N. Lam, L. Zhang, D. Ruan, E. Gad, Contact forces generated by hailstone impact, *Int. J. Impact Eng.*, 84 (2015) 145-158.
- [25] S. Perera, N. Lam, M. Pathirana, L. Zhang, D. Ruan, E. Gad, Deterministic solutions for contact force generated by impact of windborne debris, *Int. J. Impact Eng.*, 91 (2016) 126-141.
- [26] Barnes Group Inc, Bowman Distribution Engineering Department Hand Book, Fastener Facts, Cleveland- Ohio, (1989).
- [27] S.K. Samantaray, S.K. Mittal, P. Mahapatra, S. Kumar, Assessing the flexion behavior of bolted rail joints using finite element analysis, *Eng. Fail. Anal.*, 104 (2019) 1002-1013.
- [28] K. Aliakbari, N. Safarzadeh, S.S. Mortazavi, Analysis of the crankshaft failure of wheel loader diesel engine, *Int. J. Eng.*, 31(3) (2018) 473-479.
- [29] V. Infante, J.M. Silva, M.A.R. Silvestre, R. Baptista, Failure of a crankshafts of an aeroengine: a contribution for an accident investigation, *Eng. Fail. Anal.*, 35 (2013) 286-293.
- [30] A. Akyel, M.H. Kolstein, F.S.K. Bijlaard, Fatigue strength of repaired welded connections made of very high strength steels, *Eng. Struct.*, 161 (2018) 28-40.